JOURNAL OF AIRCRAFT
Vol. 39, No. 2, March–April 2002

Control of Leading-Edge Vortex Breakdown by Trailing Edge Injection

Anthony M. Mitchell,* Didier Barberis,† Pascal Molton,† and Jean Délery‡
ONERA, 92190 Meudon, France

The goal of this research is the control of the vortex breakdown locations over sharp-edged, slender, delta wings at high angles of attack. Water tunnel tests of a 75-deg delta wing examined symmetric and asymmetric trailing-edge jet injection as a method to control and delay the leading-edge vortex breakdown locations. These tests were accomplished at angles of attack between 20 and 40 deg at freestream velocities of 10 and 20 cm/s. Flow visualization data provide a description of the leading-edge vortices and of the vortex breakdown locations. The results demonstrate the ability of symmetric and asymmetric trailing-edge jet injection to control the leading-edge vortex breakdown locations. However, elevated trailing-edge injection mass flow rates create dramatic negative influences and accelerate vortex breakdown, especially for asymmetric flow control cases.

Nomenclature

A_j	=	nozzle exit surface area
C_μ	=	momentum coefficient, $Q_m V_j / q_\infty S$
c	=	root chord length
Q_m	=	injection mass flow rate, $\rho A_j V_j$
Re_c	=	Reynolds number with respect to root chord
S	=	wing planform area
s^*	=	local semispan
U_∞	=	freestream velocity
V_j	=	nozzle exit velocity
V_R	=	velocity ratio, V_j / U_∞
X, Y, Z	=	Cartesian coordinates with origin at the apex
X_b/c	=	nondimensional vortex breakdown location from wing apex
α	=	angle of attack
Λ	=	sweep angle

Introduction

THE development of extremely maneuverable fighter aircraft and missiles has pushed flight regimes to higher angles of attack and has increased interest in the study of three-dimensional separated flows. The delta wing design has become the prominent configuration used by combat aircraft manufacturers worldwide. A distinguishing feature of the delta wing flowfield, at moderate to high angles of attack, is the formation of several vortical structures over the suction surface.[1] The most prominent of these vortical structures, called leading-edge vortices, form along the sharp, leading edges of delta wings. The axial velocity component in the leading-edge vortex core can attain values as high as three times the freestream velocity.[2] At high angles of attack, these leading-edge vortices produce 30–60% of the total lift of a delta wing.[3] Therefore, delta wings have a significant advantage in total lift forces at high angles of attack, when compared with other wing designs. The vortex dynamics are influenced by several delta wing parameters including leading-edge geometry, wing thickness, and sweep angle, as well as freestream conditions and angle of attack.[4]

Well-organized leading-edge vortices exist until a sudden disorganization of the vortical structure (vortex breakdown) occurs. Several theories governing vortex breakdown have been proposed, although none is universally accepted.[5–9] In general, the vortex breakdown phenomena can be characterized by a rapid deceleration of both the axial and swirl components of velocity and a dramatic expansion of the vortex core.[9] During the breakdown process, the axial velocity component rapidly decreases until it reaches a stagnation point and/or becomes negative on the vortex axis. This stagnation point, known as the breakdown location, is unsteady and oscillates about some mean position.[8,10–12] As angle of attack is increased, the vortex breakdown location continually moves upstream over the delta wing (from downstream of the trailing edge toward the apex).

During the past 40 years, numerous theoretical, experimental and computational studies have been published, at ONERA and around the world, concerning the physics of vortical flow and vortex breakdown. However, there is limited information on trailing-edge injection as a method for control of the leading-edge vortices of a delta wing. Trailing-edge flow control techniques take advantage of existing propulsion systems to provide both energized flow and additional mass flow rates to manipulate the vortex breakdown locations. Although many studies have demonstrated the effectiveness and efficiency of flow control techniques situated near the apex or leading edges of delta wings, implementation of trailing-edge techniques could prove to be more commercially viable for real applications. Therefore, this present effort began with an examination of four previous trailing-edge flow control studies.

Helin[4] studied a 60-deg delta wing with a chord of 152.4 mm, a thickness of 6.35 mm, and a wingspan at the trailing edge of 176 mm. The tests were performed at angles of attack of 0, 10, 20, and 30 deg. Each of the two trailing-edge nozzles had an area of 80.645 mm^2 and an aspect ratio of 8. The nozzles were oriented parallel to the wing, and velocity ratios V_R were varied from 0 to 8. At angles of attack of 20 and 30 deg with a velocity ratio of 8, the breakdown location was delayed 17–18% of the chord beyond the no-blowing case.

Nawrocki[13] extended this study to include symmetric and differential injection as well as horizontally vectored trailing-edge nozzles. At the same angles of attack and velocity ratios examined by Helin,[4] Nawrocki observed a downstream displacement of the breakdown location due to symmetric trailing-edge injection of

Presented as Paper 99-3202 at the 17th Applied Aerodynamics Conference, Norfolk, VA, 28 June–1 July 1999; received 27 February 2000; revision received 20 June 2000; accepted for publication 29 November 2001.

*Exchange Engineer, Fundamental and Experimental Aerodynamics Department, 8 rue des Vertugadins; currently Assistant Professor, Department of Aeronautics, U.S. Air Force Academy, HQ USAFA/DFAN, 2354 Fairchild Drive Suite 6F49, U.S. Air Force Academy, Colorado 80840-6222. Senior Member AIAA.

†Research Engineer, Fundamental and Experimental Aerodynamics Department, 8 rue des Vertugadins.

‡Head, Fundamental and Experimental Aerodynamics Department, 8 rue des Vertugadins. Senior Member AIAA.

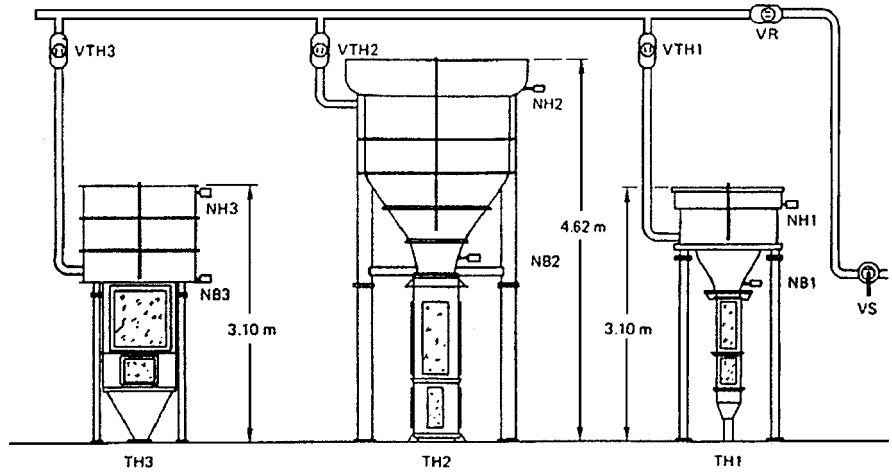

Fig. 1 Schematic of the water tunnels at ONERA Châtillon; TH2 is the center tunnel.

12–14% of the chord.[13] Differential injection results were not presented; however, with both nozzles vectored 45 deg to the starboard, the starboard breakdown location was delayed 45% of the chord beyond the no-blowing case. The portside breakdown location, apparently, remained unchanged. These results demonstrated the sensitivity of the breakdown location to the nozzle angle and the ability to individually control one of the vortex breakdown locations.

Shih and Ding[14] pursued this concept of vectored trailing-edge injection using a model that was significantly thicker than the previous models. They accomplished both static and pitching studies on a 60-deg delta wing model with a 130-mm chord, a wingspan of 151 mm, and a thickness of 25.4 mm. Their trailing-edge nozzles were much larger than those in previous tests, each with an area of 249.4 mm^2 and an aspect ratio of 9.6. These tests were accomplished at angles of attack from 10 to 35 deg. The nozzles were initially oriented parallel to the wing, and velocity ratios V_R were varied from 0 to 7.3. The largest delay in the breakdown location occurred at a velocity ratio of 7.3, which displaced the breakdown location approximately 10% of the chord downstream of the no-blowing case throughout the full range of angles of attack.

The velocity ratio was then fixed at 7.3, and the influence of various blowing angles was observed with the nozzles vectored from +30 to −45 deg (positive being upward). The largest delays were observed with the nozzles vectored 45 deg downward. At $\alpha = 15$ deg, the breakdown location was delayed 50% of the chord beyond the no-blowing case. At $\alpha = 25$ deg, the breakdown location was delayed 37.5% of the chord. The study also included an asymmetric trailing-edge nozzle setup in which the portside nozzle was deflected −30 deg and the starboard nozzle was deflected +30 deg. The downward deflected jet delayed the vortex breakdown location approximately 22% of the chord, whereas the upward injecting jet showed little favorable effect and caused no appreciable delay. These results also demonstrate that asymmetric trailing-edge flow control can provoke robust asymmetric vortex breakdown.

Vorobieff and Rockwell[15,16] examined multiple actuator control methods using leading-edge flaps and trailing-edge injection. This experiment was conducted on a pitching semispan delta wing model with a 75-deg sweep, a root chord of 243 mm, a thickness of 12.7 mm, and a semispan width of 65.11 mm. The blowing system consisted of 37, 0.8-mm-diam orifices along the trailing edge oriented 30 deg below the wing surface. The total area of the nozzles was 18.3 mm^2, and the configuration is significantly different from the three previous studies. Continuous injection was used at a velocity ratio of 4, although it was only implemented for a portion of the pitching cycle of the wing. The results indicated the ability to displace the vortex breakdown location downstream approximately 16% of the root chord.

This study examines the ability of various trailing-edge injection mass flow rates to manipulate the vortex breakdown locations. The current water tunnel tests validate the results obtained by Helin,[4] Nawrocki,[13] and Shih and Ding.[14] The results also extend the analysis to higher trailing-edge injection velocity ratios in both asymmetric and symmetric blowing configurations.

Water Tunnels

The vertical water tunnel TH2 was utilized during these tests and has a square test section with cross section dimensions of 45 cm per side and a length of 1.2 m (1.9 m if the test section is extended to the ground level at lower freestream velocities). A water reservoir of 6600 liter, with its top lip situated 4.62 m above the floor, rests on top of a columnar structure containing the test section (Fig. 1). A converging nozzle with a high contraction ratio assures a uniform velocity in the test section. A honeycomb filter exists at the start of the converging section upstream of the test section to eliminate turbulent flow, which can develop in the reservoir. At ground level, a control valve is adjusted to control the flow of the water. As the valve is opened, velocity is created in the test section due to the gravitational acceleration of the water from the elevated reservoir. When the 150-mm-diam valve is utilized, the maximum attainable velocity in the test section is 25 cm/s ($Re_c = 10^5$). If the 400-mm-diam valve is regulated, the maximum attainable velocity is 150 cm/s ($Re_c = 6 \times 10^5$). During these tests, the smaller valve was used, resulting in run times varying from 100 s at 25 cm/s to approximately 4 min at 5 m/s. During each run, however, the mass flow in the test section can decrease 20% between the start and the end of the run due to a reduction in the total head of water as the reservoir is emptied. Neither pressure measurements nor fluctuations of the mass flow rate were measured in the test section.

To minimize the changes in mass flow during each test run, the duration of each test is limited. After each run, the reservoir is refilled to the same level and the water stabilized to eliminate air bubbles and surface waves, which are generated during the refilling of the basin. Flow is established in the test section, and then each test begins as the water level passes a specified point. Similarly, the end of each run occurs as the water level passes an indicated minimum level. These precautions are accomplished to maintain a more constant freestream velocity in the test section during each run. Even after implementing these precautions, there is approximately a 9% change in the mass flow rate in the test section between the start of each test run and its conclusion.

Isolated systems for injection and suction are available for use with each of the water tunnels. Two separate circuits are available for fluid injection, each using three rotameters to provide mass flow rates from 1 to 2100 cm^3/s. A third circuit, which includes a pump, is available to provide suction at mass flow rates from 1 to 3200 cm^3/s.

Models can be mounted in the test section by stings attached to the sidewall of the test section or by stings mounted from downstream of the test section. Special stings exist to permit rotational and oscillatory movement of the models. In these tests, the pressure

side of the delta wing model was attached to a sting mounted to the rear wall of the test section (Fig. 2).

Model

The 75-deg delta wing model has a chord of 400 mm and a thickness of 5 mm. The wingspan at the trailing edge is 216 mm. The leading edges and the trailing edge are beveled at 15 deg (Fig. 3). The model has 10 small ports near the apex on the suction surface for the injection of colored dyes to visualize the flow around the delta wing. There are five dye nozzles along each leading edge: one near the apex, the others at 30, 50, 90, and 130 mm from the apex, respectively.

For this study of trailing-edge injection, a settling chamber and two rectangular nozzles are affixed to the pressure surface of the delta wing model. Both nozzles are mounted flush with the trailing edge of the wing and are oriented parallel to the suction surface of the model, that is, no thrust vectoring. Individual nozzle exit surface areas A_j are 1.209 cm^2 and have aspect ratios of 8.47 (Fig. 3). Each of the nozzles is attached to an independent fluid injection circuit, which allows for symmetric and asymmetric flow control configurations.

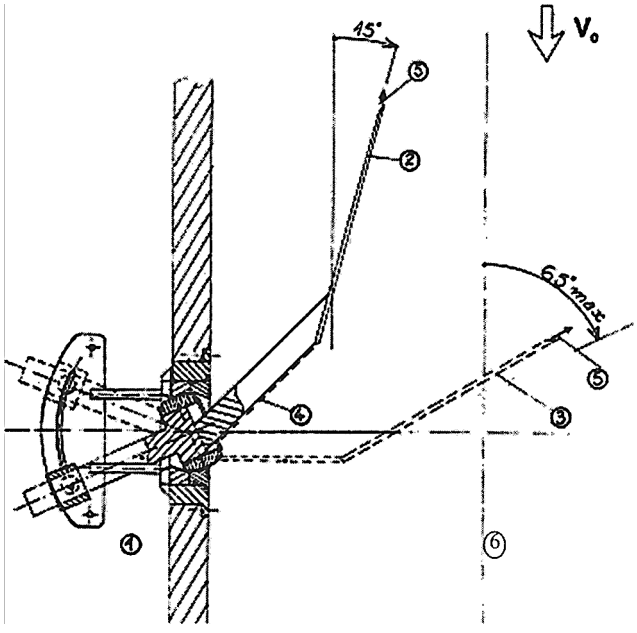

Fig. 2 Schematic of the experimental configuration as installed in TH2: 1, mechanism for adjusting the angle of attack of the model; 2, delta wing model at $\alpha = 15$ deg; 3, delta wing model at $\alpha = 65$ deg; 4, aerodynamic sting, and 5 apex of the delta wing model.

Data Acquisition and Uncertainty

Reservoirs of silicon-based colored dyes, with densities equal to that of water to eliminate buoyancy effects, are situated near the top of each water tunnel. The dyes are transported, by gravitational force, to a panel of valves that regulates the mass flow emitted from the ports on the surface of the delta wing near the apex and along the leading edges. The ensuing streaklines of dye are illuminated from both sides of the test section with theater spotlights. The resulting flow visualizations provide a qualitative description of the leading-edge vortices and enable the identification of the vortex breakdown locations. The various tests are recorded with a Sony digital video camera at a rate of 25 frames/s with the camera positioned perpendicular to the front of the test section and at the same height as the model. Every effort is made to minimize the amount of colored dye injected at each port along the model while providing sufficient color to visualize the phenomena. This is not a quantitative process, and repeatability is the goal throughout a series of tests; thus, once a satisfactory setting is determined for a given flow speed, the setting is fixed.

In spite of these precautions, some drift in the time-dependent vortex breakdown location was observed, especially for angles of attack below 32 deg. This downstream drift of the vortex breakdown locations is partially due to the influence of the colored dyes being injected into the flow near the apex and along the model's leading edges and partially due to the proximity of the vortex breakdown to the trailing edge of the delta wing. During the course of a test, the total head of the colored dye does not change significantly. As the dye is injected around the model, the height of the dye in the reservoir changes only approximately 0.5 cm during a run. On the other hand, the total head of the water used to create the freestream velocity in the test section does change significantly. The height of the water in the reservoir above the test section decreases 1.5 m during a test; therefore, the ratio of the momentum of the colored dye injected around the model into the freestream velocity increases as the water level of the tunnel decreases. As the momentum of the colored dye injected into the flow increases, it has stronger leading-edge blowing

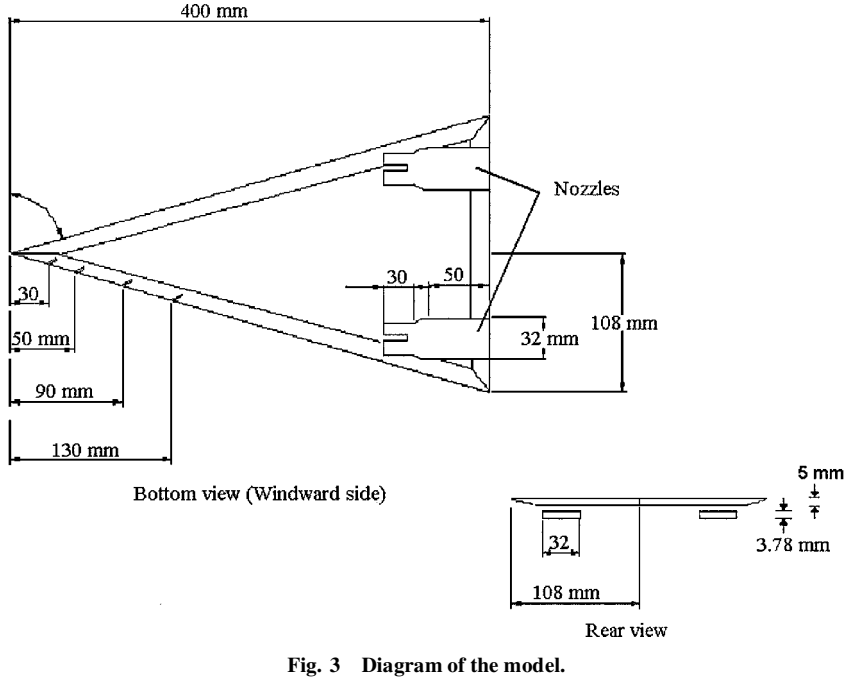

Fig. 3 Diagram of the model.

influences, a flow control technique known to displace the vortex breakdown location downstream. Consequently, the influence of the injection of colored dyes in this manner was observed as a downstream drift in the breakdown location throughout all of the tests up to an angle of attack of 32 deg.

At incidences larger than 32 deg, the breakdown location stabilized and no longer drifted as a function of time. Previous studies have shown that the vortex breakdown location is more sensitive to irregularities in the flow and exhibits greater oscillations at locations near the trailing edge than farther upstream. This is frequently attributed to the vortex strength and the influence of adverse pressure gradient at the trailing edge. Therefore, as the angle of attack increases, the breakdown location moves farther upstream and is less sensitive to the influence of the trailing edge. Both the adverse pressure gradient at the trailing edge and the vortex strength are higher and overcome the weak jetlike influence of the colored dye being emitted from the leading edges near the wing apex.

Measurements of the streamwise distance of the breakdown locations (port and starboard) from the apex of the delta wing, X_b, were obtained directly from the frame-by-frame recorded video images. These values were then divided by the respective observed root chord c at each angle of attack, also measured directly from the video images, resulting in a nondimensional length X_b/c. The angle between the video camera and the model is neglected because all of the lengths measured are obtained from the same video frame. The angle between the suction surface of the delta wing model and the axis of each leading-edge vortex remains constant at approximately 6 deg throughout the incidence range examined during these tests. Because this angle is small, its influence on the breakdown location is neglected, and measurements are obtained from reference marks on the suction surface of the delta wing. Measurement uncertainty for the identification of the vortex breakdown locations is on the order of $0.02c$.

All of the data presented in this paper are raw data that have not been corrected or adjusted for tunnel wall effects. The delta wing model at various angles of attack in the water tunnel does have relatively large percentages of tunnel blockage. At $\alpha = 27$ deg, a blockage of 9.68% was calculated, whereas at $\alpha = 35$ deg, the blockage was 12.24%. Therefore, the tunnel walls will have an influence on the flowfield and the vortex breakdown location, changing the effective angle of attack of the model. In addition to the blockage directly due to the delta wing model, the sting and model support can also influence the flowfield and the vortex breakdown location. During these tests, neither flow visualization nor measurements were accomplished around the support system to examine the interference and blockage effects.

Additionally, the high-injection mass flow rates from the trailing-edge jets will have an influence on the tunnel walls and the flow downstream of the model. The model was mounted along the tunnel centerline, and the jets were mounted flush on the pressure surface of the delta wing model. Therefore, the injected flow merges with the freestream flow at the incidence angle of the model. The jets were mounted flush with the trailing edge of the wing, and thus, the interaction of the jets with the tunnel walls was downstream of the model. It is likely that the jets disturbed the flow and the tunnel boundaries. The influence of the jets on the tunnel boundaries was not analyzed, except for the comparisons between the blowing and no-blowing configurations.

Results

The results of the influence of trailing-edge injection reported here were obtained while the model was fixed at an angle of attack of 35 deg. The tests were accomplished at a freestream velocity of 10 cm/s ($Re_c = 4 \times 10^5$). Trailing-edge injection for each of the nozzles was implemented at velocity ratios V_R of 0, 5, 10, and 15. At $U_\infty = 10$ cm/s, the corresponding injection mass flow rates associated with these velocity ratios are 60.45, 120.9, and 181.35 cm^3/s.

In previous studies, the delta wing models and corresponding nozzle areas are all different, thus complicating direct comparisons of velocity ratios and their influence on the breakdown locations. Different authors have used various definitions of the nondimensional momentum coefficients, making direct comparison of the results difficult. Momentum coefficients have been recalculated for each of these tests using the definition of C_μ presented in the Nomenclature. The maximum momentum coefficients are 1.537 (Refs. 4 and 13), 5.256 (Ref. 14), and 0.2643 (Refs. 15 and 16). A maximum velocity ratio equal to 8 was examined, which is well below those examined in the current experiments, although Shih and Ding[14] examined a maximum momentum coefficient larger than the current maximum value of 2.539. In this study, the corresponding momentum coefficients C_μ, with only one nozzle active (asymmetric cases), are $C_\mu = 0.141$, 0.564, and 1.269 for $V_R = 5$, 10, and 15, respectively. When both nozzles are active (symmetric case), $C_\mu = 0.282$, 1.128, and 2.539 for $V_R = 5$, 10, and 15, respectively.

Water was injected in an open-loop system before the flow in the water tunnel was initiated. Therefore, the injection was well established before data were recorded and time lags and unsteady effects were eliminated. Each of the two trailing-edge jets was individually controlled to permit symmetric and asymmetric flow control. Initially, symmetric jet injection was examined using both of the nozzles with identical jet velocity ratios. The asymmetric configurations were accomplished by stopping the jet injection on one side of the wing or the other and then examining the resulting effects on both vortex breakdown locations.

No Flow Control

The uncontrolled vortex breakdown locations were first examined to quantify the observations of the breakdown locations in the water tunnel. Results demonstrate asymmetry between the port and starboard vortex breakdown locations. This could be due to a slight yaw angle of the wing with respect to the freestream velocity in the test section, which favors the portside breakdown. Frame by frame analysis of the vortex breakdown locations (port and starboard) revealed an oscillation around a mean breakdown location with amplitude of approximately 5% of the root chord. These results confirm previously published observations in both wind and water tunnels.[10,17]

The time-averaged values of the breakdown locations $\bar{X}_b/c$ without flow control are plotted in Fig. 4, for a number of different angles of attack. Error bars represent the amplitude of the oscillating time-dependent breakdown locations. Each plotted mean value is obtained from more than 1500 time-dependent data points (approximately 60 s of data at 25 frames/s). The nondimensional breakdown location X_b/c data are defined such that, when $X_b/c = 1$, the breakdown location is at the trailing edge of the delta wing. A measurement of $X_b/c = 0$ indicates a breakdown location at the apex or leading edge of the delta wing.

One observes the forward shift of the mean breakdown location as the incidence angle is increased from 27 to 40 deg. Additionally, the data at identical angles of attack and different freestream velocities confirm previous studies of delta wings with sharp leading edges. The sharp leading edges of the delta wing fix the primary separation line, and the Reynolds number effects are negligible.

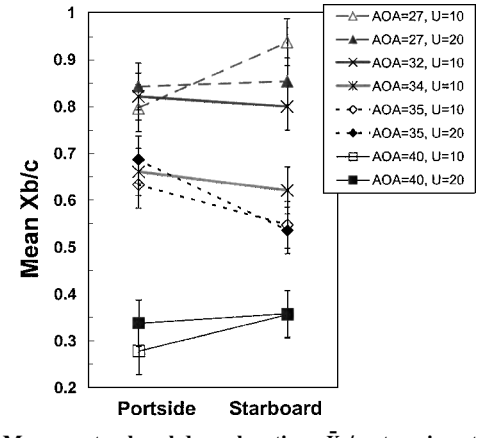

Fig. 4 Mean vortex breakdown locations $\bar{X}_b/c$ at various test conditions, no flow control.

Asymmetric Flow Control

The uncontrolled mean vortex breakdown locations obtained at $\alpha = 35$ deg and $U_\infty = 10$ cm/s (Fig. 4) will be compared to the results presented at the same test conditions for both asymmetric and symmetric trailing-edge injection configurations. The mean vortex breakdown location data are plotted in Figs. 5a, 5b, and 6 for three trailing-edge injection velocity ratios: portside blowing only (Fig. 5a), starboard blowing only (Fig. 5b), and symmetric blowing

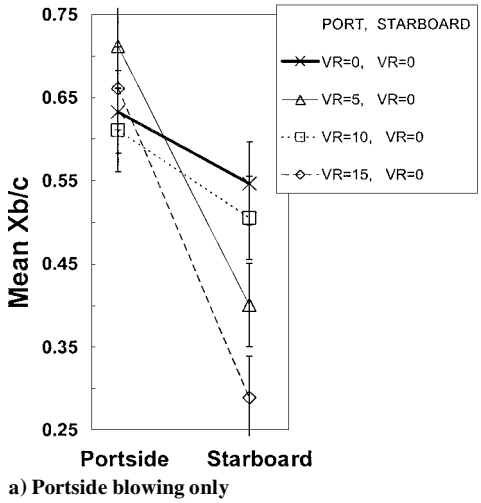

a) Portside blowing only

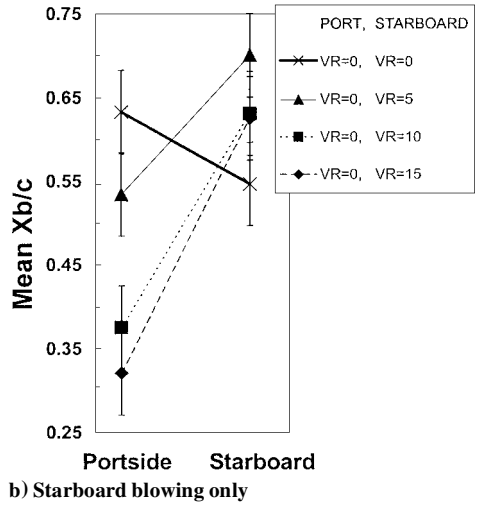

b) Starboard blowing only

Fig. 5 Mean vortex breakdown locations $\bar{X}_b/c$ for asymmetric trailing-edge injection.

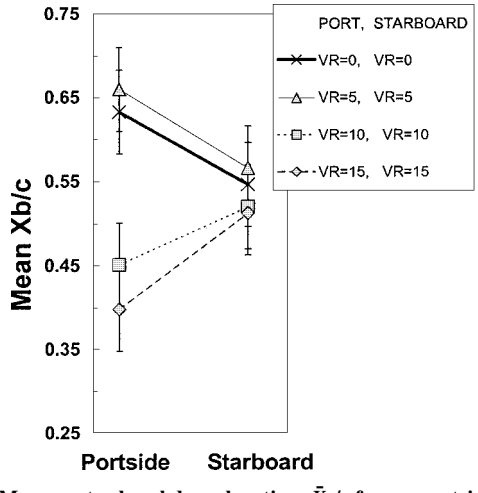

Fig. 6 Mean vortex breakdown locations $\bar{X}_b/c$ for symmetric trailing-edge injection.

from both nozzles (Fig. 6). In each of these curves, the points indicated by an × and connected with a thick solid line, represent the mean no-blowing case from Fig. 4.

Figure 5a demonstrates the influence of asymmetric trailing-edge injection from the portside nozzle for three different velocity ratios. When $V_R = 5$, the mean portside vortex breakdown location, $\bar{X}_b/c = 0.71$, shifts 8% of the chord downstream from its uncontrolled mean location. Equally interesting is the unexpected adverse influence of the asymmetric portside injection on the starboard vortex breakdown location. In this case, the mean starboard breakdown location, $\bar{X}_b/c = 0.40$, shifts 15% of the chord upstream from its uncontrolled mean location. When the velocity ratio is increased to 10, the mean portside vortex breakdown location, $\bar{X}_b/c = 0.61$, shifts 2% of the chord upstream of its uncontrolled mean location. The mean starboard breakdown location, $\bar{X}_b/c = 0.51$, is displaced 4% of the chord upstream of its uncontrolled mean location. Finally, when the velocity ratio is increased to 15, the mean portside vortex breakdown location, $\bar{X}_b/c = 0.66$, is moved 3% of the chord downstream of the uncontrolled mean breakdown location. The uncontrolled mean starboard breakdown location, $\bar{X}_b/c = 0.29$, shifted 25% of the chord upstream.

All three asymmetric portside injection cases have negative slopes between the mean portside and starboard breakdown locations. The controlled, mean, portside breakdown locations are always situated farther downstream than the corresponding uncontrolled, mean, starboard locations. This indicates the desired downstream displacement of the controlled vortex breakdown due to trailing-edge injection and an adverse influence on the uncontrolled breakdown location. At the velocity ratio of 10, the mean portside breakdown location does not conform to the trends observed in the other data; however, it is only 2% upstream of the reference location, well within the error bars of the data depicting the amplitude of the oscillating time-dependent breakdown locations. This small difference ensures continuity in the general trends of the displacement of the controlled and uncontrolled breakdown locations.

Figure 5b presents similar trends to those observed in Fig. 5a, only now the asymmetric trailing-edge injection is applied on the starboard side of the wing while the portside vortex is not controlled. For all three velocity ratios, the slope of the line connecting the mean portside and starboard breakdown locations is positive; therefore, the starboard mean breakdown locations are always situated farther downstream than the corresponding uncontrolled, portside locations. This demonstrates the desired downstream displacement of the controlled vortex breakdown due to trailing-edge injection and an adverse influence on the uncontrolled breakdown location. At $V_R = 5$, the mean starboard breakdown location, $\bar{X}_b/c = 0.70$, is shift downstream by 15% of the chord from its uncontrolled mean location. The uncontrolled mean portside breakdown location, $\bar{X}_b/c = 0.53$, was adversely moved closer to the wing apex by 10% of the chord. With asymmetric trailing-edge injection at $V_R = 10$, the mean starboard breakdown location, $\bar{X}_b/c = 0.63$, is 9% of the chord downstream from its uncontrolled mean location. The uncontrolled portside breakdown location, $\bar{X}_b/c = 0.37$, has shifted closer to the wing apex by 26% of the chord. Finally, at a $V_R = 15$, the mean starboard breakdown location, $\bar{X}_b/c = 0.63$, has been delayed downstream 9% of the chord from its uncontrolled mean location. The portside breakdown location, $\bar{X}_b/c = 0.32$, has shifted upstream 31% of the chord from its uncontrolled mean location.

The current results (Figs. 5a and 5b) demonstrate that the effect of asymmetric injection is consistent in delaying the vortex breakdown location of the controlled vortex for all velocity ratios considered. However, asymmetric injection adversely initiated early vortex breakdown of the uncontrolled vortex for all velocity ratios. These results confirm Shih and Ding's results[14] that asymmetric vortex breakdown produced by the trailing edge jet is robust. Additionally, the asymmetric trailing-edge injection demonstrated the ability of this flow control technique to influence the uncontrolled vortex breakdown location through manipulation of the trailing-edge pressure gradient. It is hypothesized that the asymmetric blowing blocks the flow on the side where it is applied, and as a result, the flow works

its way to the other side. Therefore, the local velocity increases, resulting in the upstream movement of the vortex breakdown on the uncontrolled side of the wing. This left and right asymmetry could be similar to the influence of yaw on the breakdown location. Velocity and pressure measurements were not obtained during these tests and, therefore, cannot provide sufficient proof of this observation-based hypothesis.

Symmetric Flow Control

One must examine the influence of symmetric trailing-edge injection. Figure 6 shows the observed results of symmetric trailing-edge injection through both nozzles for the three velocity ratios. At $V_R = 5$, both the port and starboard vortex breakdown locations have been slightly delayed when compared to the no-blowing case. The mean portside breakdown location is 0.66, and the mean starboard breakdown location is 0.57. Therefore, the mean breakdown locations have both been delayed downstream 3% of the chord from their uncontrolled mean location. This confirms previously published data.[4,13,14]

Current results, at $V_R = 5$, confirm that the vortex breakdown location can be displaced downstream between 5 and 10% of the root chord for the controlled asymmetric injection or symmetric injection cases without nozzle vectoring. This corresponds to the control effectiveness observed in the previous tests involving nonvectored trailing-edge injection. Note that previous papers did not discuss the influence of the flow control method on each of the leading-edge vortex breakdown locations, but instead relied on an average displacement of the vortex breakdown observed. The results of vectored trailing-edge injection were shown to influence each of the leading-edge vortices separately and to improve the effectiveness of the given velocity ratios. Vectored trailing-edge blowing cases were not studied in the current experiments.

However, when $V_R = 10$, both the port and starboard vortex breakdown locations have been adversely shifted closer to the wing apex than in the no-blowing case. The mean portside and starboard breakdown locations are equal to 0.45 and 0.52, respectively. Therefore, the mean breakdown locations have been shifted upstream 18 and 3% of the chord from their uncontrolled mean location. Finally, the results of symmetric trailing-edge injection through both nozzles at $V_R = 15$ demonstrate that both the port and starboard vortex breakdown locations are even farther upstream than their respective no-blowing locations. The respective mean portside and starboard breakdown locations are 0.40 and 0.51. Therefore, the mean breakdown locations have shifted upstream 23 and 4% of the chord from their uncontrolled mean location.

Previously published results suggest that, as the injection velocity ratio increases, the vortex breakdown location is displaced farther downstream. Data from this study demonstrate that increasing the mass flow rate of symmetric trailing-edge injection continues to delay the vortex breakdown location up to a velocity ratio between 5 and 10. When the velocity ratio is above this range, the symmetric trailing-edge injection induces an adverse effect on the vortex breakdown locations causing premature vortex breakdown. As the injection velocity ratio is increased, the subduing influence on the adverse pressure gradient at the trailing edge is reversed, and the vortex breakdown is promoted. These results obtained at higher velocity ratios contradict the assumption that increasing trailing-edge injection mass flow rates will induce larger downstream displacement of the vortex breakdown locations.

In the asymmetric blowing cases, the flow on the controlled side is blocked by stronger adverse pressure gradients as the injection velocities are increased. The flow works its way to the other side to lessen the impact of the larger adverse pressure gradient. However, with the application of symmetrical blowing, the flow cannot move from one side of the wing to the other, but is completely blocked and causes the flow to spill over more toward the suction surface. The highest trailing edge injection velocity creates the strongest adverse pressure gradient along the entire the trailing edge and results in the upstream movement of the vortex breakdown location.

Conclusions

Control of the leading-edge vortex breakdown location over a delta wing was accomplished utilizing both symmetric and asymmetric trailing-edge injection. Trailing-edge injection manipulated the vortex breakdown locations over a delta wing, although its effectiveness is highly dependent on the velocity ratios applied, as well as the configuration and orientation of the jets.

The mean vortex breakdown locations under the influence of asymmetric trailing-edge injection remain stable throughout the experiment and are consistent for all angles of attack tested. Asymmetric trailing-edge injection was consistent in delaying the vortex breakdown location of the controlled vortex for all velocity ratios considered. However, it adversely initiated early vortex breakdown of the uncontrolled vortex for all velocity ratios. Not only did this indicate adverse control effects, but also demonstrated the ability of asymmetric trailing-edge injection to influence the uncontrolled vortex breakdown location.

Symmetric trailing-edge injection results at high-velocity ratios demonstrate that augmenting the velocity ratio will not continue to displace the vortex breakdown location favorably. There is an upper limit on the effective velocity ratio that can provide positive vortex breakdown control. After this limit is attained, the symmetric trailing-edge injection has an adverse effect on the vortex breakdown location and causes premature breakdown.

Acknowledgments

The authors would like to express their sincerest thanks to Marc Gallon, without whom these tests would never have been accomplished. The authors would also like to thank the U.S. Air Force Institute of Technology/Civilian Institutions, the U.S. Air Force Academy and ONERA/Fundamental and Experimental Aerodynamics Department for their support of this international cooperative effort.

References

[1]Délery, J., "Physics of Vortical Flows," *Journal of Aircraft*, Vol. 29, No. 5, 1992, pp. 856–876.

[2]Werlé, H., "Sur l'éclatement des tourbillons," ONERA, Note Technique No. 175, Chatillon, France, July 1971.

[3]Wentz, W. H., Jr., and Kohlman, D., "Vortex Breakdown on Slender Sharp-Edged Wings," *Journal of Aircraft*, Vol. 8, No. 3, 1971, pp. 156–161.

[4]Helin, H. E., "Effects of Trailing Edge Jet Entrainment on Delta Wing Vortices," *AIAA Journal*, Vol. 34, No. 4, 1994, pp. 802–804.

[5]Hall, M. G., "Vortex Breakdown," *Annual Review of Fluid Mechanics*, Vol. 4, 1972, pp. 195–218.

[6]Leibovich, S., "The Structure of Vortex Breakdown," *Annual Review of Fluid Mechanics*, Vol. 10, 1978, pp. 221–246.

[7]Sarpkaya, T., "On Stationary and Travelling Vortex Breakdowns," *Journal of Fluid Mechanics*, Vol. 45, Pt. 3, 1971, pp. 545–559.

[8]Nelson, R. C., "Unsteady Aerodynamics of Slender Wings," *Aircraft Dynamics at High Angles of Attack: Experiments and Modeling*, AGARD-R-776, 1991, pp.1-1–1-26.

[9]Délery, J., "Aspects of Vortex Breakdown," *Progress in Aerospace Sciences*, Vol. 30, Great Britain, Jan. 1994, p. 1–59.

[10]Mitchell, A. M., Barberis, D., and Délery, J., "Oscillation of Vortex Breakdown and Control of the Time-Averaged Location by Blowing," *AIAA Journal*, Vol. 38, No. 5, 2000, pp. 793–803.

[11]Seginer, A., and Salomon, M., "Augmentation of Fighter Aircraft Performance by Spanwise Blowing over the Wing Leading Edge," NASA-TM-84330, March 1983.

[12]Menke, M., and Gursul, I., "Self-Excited Oscillations of Vortex Breakdown Location over Delta Wings," AIAA Paper 97-0742, Jan. 1997.

[13]Nawrocki, D., "Differential and Vectored Trailing Edge Jet Control of Delta Wing Vortices," AIAA Paper 95-0008, Jan. 1995.

[14]Shih, C., and Ding, Z., "Trailing Edge Jet Control of Leading-Edge Vortices of a Delta Wings," *AIAA Journal*, Vol. 34, No. 7, 1996, pp. 1447–1456.

[15]Vorobieff, P., and Rockwell, D., "Multiple-Actuator Control of Vortex Breakdown on a Pitching Delta Wing," *AIAA Journal*, Vol. 34, No. 10, 1996, pp. 2184–2186.

[16]Vorobieff, P., and Rockwell, D., "Vortex Breakdown on Pitching Delta Wing: Control by Intermittent Trailing-Edge Blowing," *AIAA Journal*, Vol. 36, No. 4, 1998, pp. 585–589.

[17]Gursul, I., and Yang, H., "On Fluctuations of Vortex Breakdown Location," *Physics of Fluids*, Vol. 7, No. 1, 1995, pp. 229–231.